On-chip terahertz systems for spectroscopy and imaging

J. Cunningham, M.B. Byrne, C.D. Wood and L. Dazhang

A review is conducted of recent advances in the technology and applications of on-chip integrated terahertz systems, in which pulses of terahertz frequency radiation are generated by a photoconductive material, guided through a planar waveguide, and then detected coherently by photoconductive detection. These integrated systems are highly compact compared with typical free-space time domain terahertz spectroscopy systems, and allow much smaller sample volumes to be investigated, since they concentrate the propagating terahertz field to a length-scale far smaller than the diffraction limit. How both time-domain spectroscopy and imaging can be acheived using on-chip terahertz systems is discussed, along with some potential future applications for on-chip systems in the terahertz spectroscopy of single nanostructures.

Introduction: In the technique of free-space terahertz time domain spectroscopy (THz-TDS) [1], few- or single-cycle pulses of terahertz radiation are generated by ultrafast (typically 10–100 fs) laser excitation of either a photoconductor (typically a semiconductor), or an electro-optic material, followed by collection of the emitted THz radiation by parabolic mirrors, and subsequent collimation and/or focusing of the radiation onto a sample. The radiation, modified by its interaction with the sample, is collected either in transmission or reflection geometry, and then focused onto a detector (either a photoconductive or electro-optic material). Time-domain detection then proceeds by making a time-delayed portion of the original ultrafast laser beam co-incident with the terahertz pulse at the detector. These two co-incident pulse trains form a convolution signal, consisting of either a photocurrent (photoconductive detection) [2], or a difference signal on two balanced photodiodes; the latter measures the polarisation state of the laser beam, which is affected by the co-incident terahertz electric field owing to the Pockels effect (electro-optic detection) [3]. In either case, the arrival time of the delayed portion of the laser pulse is altered while the detector signal is monitored, allowing the time-dependent electric field of the THz pulse to be mapped out. This technique, while suited to the investigation of a wide range of material systems, has several limitations as described below.

1. *Sample size*. The minimum diameter of the focused THz beam is restricted by diffraction, so that measurements on samples with a size $<\lambda_{THz}$ are problematic, since some portion of the THz beam will 'leak' around the edges of the sample. If a restricting aperture technique is used to circumvent this leakage, to ensure that the entire beam interacts with the sample, THz power is wasted, since some portion of the beam is reflected by the aperture. Bandwidth is also reduced by the aperture, with lower frequency components of the THz pulse being cut-off.

2. *Frequency resolution*. The frequency resolution of a spectroscopy system determines the accuracy with which sharp spectral features can be recorded. In a typical THz-TDS measurement, a Fourier transform is taken of the time-domain signal both with and without the sample placed in the beam path. Evaluation of the real and imaginary parts of both Fourier spectra then yields the frequency-dependent absorption coefficient and refractive index of the sample [4]. The resolution of the absorption and refractive index so obtained is limited (typically to a few tens of gigahertz) by the available time-window for the time-domain measurement; in order that a clean frequency-domain spectra is obtained, multiple THz path reflections in the emitter, detector, and any other components in the beam path, must be excluded from the time-domain trace.

3. *System size*. The overall system size (and indeed cost) of free-space THz-TDS systems was for many years dictated by the bulky 800 nm Ti:sapphire laser system used for ultrafast excitation in the THz emission and detection processes. With the advent of compact, cheaper, fibre lasers operating at 1.55 μm, and photoconductive materials suited to generation and detection of pulsed THz radiation using comparable wavelengths (such as Fe-InGaAs [5]), much smaller systems have become available, so that the system size is now partly restricted by the free-space optics (parabolic mirrors) required for capturing, collimating, and focusing THz radiation through the sample. Further reduction in system size is desirable, however, so that handheld THz spectroscopy systems can be made (there are strong parallels here with the progress and reduction in size of Raman spectroscopy systems seen over the last 10 years).

Each of these limitations can be addressed, to a greater or lesser extent, by the use of on-chip THz systems, in which THz pulses are generated by thin-film photoconductive switches embedded in lithographically-defined waveguides. In an on-chip THz system, the cross-sectional area occupied by the propagating electric field is many orders of magnitude smaller than the area of the focal spot in a (diffraction-limited) free-space THz-TDS system, allowing much smaller samples to be measured effectively. Furthermore, the volume of the interacting electric field in an on-chip system can be controlled, both rather directly by the bias applied to the photoconductive switches, and (somewhat less flexibly) by the geometry chosen for the waveguide. The predominant reflections in on-chip systems occur at points of impedance discontinuity in the waveguide, so on-chip systems can be easily designed to suppress reflections over very long time windows (hundreds of picoseconds), leading to a very high frequency resolution (<2 GHz) in the measurement of the absorption and the refractive index of samples.

The history of on-chip systems for transmission of terahertz pulses arguably began with the work by Auston and co-authors on photoconductive processes, and by demonstration of sub-millimetre waveguiding on amorphous silicon [6]. Such work was later extended by Grischkowsky and others, by the investigation of a range of on-chip THz waveguides [7]. A key technological step came from the integration of a photoconductive semiconductor (low-temperature grown gallium arsenide, LT-GaAs) onto low-loss dielectric substrates by the Aachen group [8], using an epitaxial lift-off process first demonstrated by Yablonovitch [9]. This decoupling of the photoconductive emitter from the substrate used for transmission was important, since one could then optimise the THz emission characteristics separately from the dielectric supporting the waveguide. The THz emission properties of LT-GaAs can be tuned by controlling the anneal temperature of LT-GaAs after growth, so that careful optimisation can be carried out to minimise the photocarrier lifetime [10]. Our group at Leeds showed that LT-GaAs could be integrated onto a dielectric for THz detection in the same chip as the emitter, allowing a fully integrated system to be built, in which an optimised photoconductive emitter and detector are joined by a THz waveguide [11].

Before we discuss on-chip terahertz waveguides in more detail, it is worth mentioning the other waveguides available in this region of the spectrum. There are many waveguides which can capture and confine the THz radiation which has been generated by a THz-TDS system and released into air, with prominent examples being suspended-wire waveguides [12], parallel-plate waveguides [13], and dielectric ribbons [14]. By contrast, in on-chip systems the THz radiation is confined to a lithographically defined metal transmission line waveguide on a dielectric surface, with the most studied examples being the coplanar-line [15], the microstrip-line [16], and the Goubau-line [17]. On-chip THz waveguides typically show higher attenuation and dispersion than the free-space waveguides, owing to the propagating electric field being predominantly confined to lossy (compared with free-space) dielectric materials. They are therefore generally unsuitable for long distance (> few centimetres) signal transmission, but they can form the basis of THz frequency circuits with, for example, passive components such as filters being integrated directly into the waveguide [11]. Furthermore, the evanescent electric field around THz current pulses propagating in on-chip waveguides can be used for both microscopy [18], and for recording vibrational absorption spectra [19]. In the following Sections we discuss both these techniques of THz spectroscopy and imaging using such on-chip waveguides, followed by some speculation over future directions which the development of on-chip THz systems are likely to take.

Spectroscopy: The first experiment we discuss, shown in Fig. 1*a*, demonstrates the use of the evanescent field above a THz on-chip system for spectroscopy. LT-GaAs was grown at 200°C, using molecular beam epitaxy, annealed *ex-situ* at 500°C for 15 minutes, and then transferred (after removal of an underlying sacrificial layer of AlAs in hydrofluoric acid) to a dielectric-coated silicon wafer. The dielectric chosen was benzocyclobutene (BCB) in this case, which can be spin coated, and has reasonably low THz absorption and loss [20] (other common choices for THz dielectric in on-chip systems include polymeric plastics such as PTFE, and quartz [17]). A thick (few hundred nanometres) layer of gold, evaporated onto the silicon wafer before dielectric deposition, acted as a backplane for the microstrip signal conductor, which was itself formed by optical lithography and subsequent metallisation (typically 20/300 nm Ti/Au) on top of the BCB.

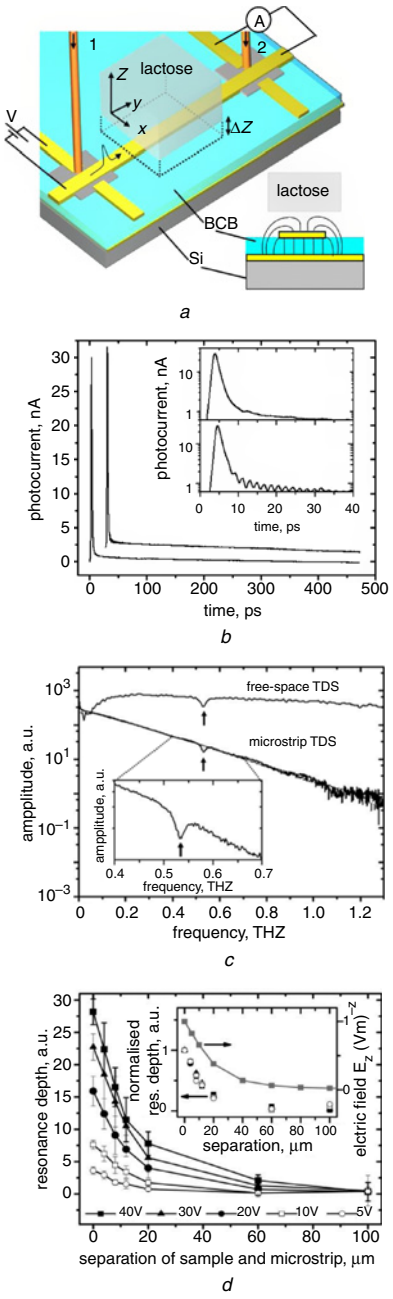

Fig. 1 *Schematic diagram showing experimental arrangement used for THz spectroscopy using on-chip systems; time-domain traces taken with lactose sample in full contact with microstrip waveguide; Fourier transforms of data shown in Fig. 1b; depth of resonance obtained from on-chip system against separation between lactose sample and waveguide*

a Schematic diagram showing experimental arrangement used for THz spectroscopy using on-chip systems.
Near-infrared laser pulses (centred at 800 nm, duration 100 fs, with repetition rate of 80 MHz) were focused onto biased regions of LT-GaAs (grey squares) for THz signal excitation, 1, and time-delayed detection, 2. A polycrystalline lactose sample was suspended over a microstrip waveguide, within the region of evanescent field (shown in cross-section), while pulses propagating along microstrip waveguide were monitored using photoconductive sampling.
b Time-domain traces taken with lactose sample in full contact with microstrip waveguide (lower main Figure and lower Inset) and reference traces taken with lactose sample well outside the region of evanescent field extended above microstrip (upper main Figure and upper Inset).
In main Figure, lactose trace has been offset on both axes for clarity.
c Fourier transforms of the data shown in Fig. 1*b*, with a free-space measurement of larger lactose pellet for comparison.
On-chip data shows similarly pronounced absorption, despite comparatively tiny interacting volume of electric field.
d Depth of resonance obtained from on-chip system against separation between lactose sample and waveguide, for different biases applied to input photoconductive switch.
Absorption resonance can be still observed for separations >50 μm.
Inset: Experimental data, rescaled by constant factor for each applied voltage, collapsed onto single line.
A 3D numerical simulation of the system (grey squares) shows predicted magnitude of the instantaneous vertical component of electric field, with similar functional form to the collapsed data (grey line is a guide to the eye).

A THz pulse was first generated by focusing an 800 nm Ti-Sapphire laser beam onto one of the LT-GaAs switches. This pulse was coupled into and along the microstrip waveguide, before being detected by a second photoconductive switch fabricated at its far end. Scanning a time delay stage changed the arrival time of a second time-delayed portion of the 800 nm beam at the second switch, and the transmitted THz pulse shape was recovered by monitoring the current generated in the second switch as this arrival time was adjusted, similar to the detection method used in free-space THz-TDS. Comparing this output signal with the input pulse shape onto the microstrip (obtained by autocorrelation at the input switch) allows us to estimate that the (quasi-TEM) mode in this microstrip system propagates with a loss of approximately 3 dB per millimetre at 1 THz [11], limiting the usable length of the microstrip to a few millimetres for reasonable applied laser power levels (<100 mW) and biases (<100 V), chosen to avoid damage to the photoconductive switches. Time-domain data showing the pulse received at the second switch is shown in Fig. 1*b*. A clear single cycle pulse is seen, with FWHM duration $\sim$1.5 ps, after passage along the microstrip. Since there are no reflections seen within the available time window of 470 ps, we can Fourier transform this entire time window, obtaining a very high frequency resolution in the Fourier transform of the data ($\sim$2 GHz).

Next, a sample of polycrystalline lactose was brought into the evanescent field above the microstrip using a piezoelectric translation stage. Fig. 1*b* shows time-domain data obtained with the lactose in full contact with the microstrip. A clear ringing in the pulse is seen, caused by interaction and absorption of frequencies from the terahertz pulse by the lactose sample. The Fourier transform of the data shows a clear single absorption resonance at 530 GHz (Fig. 1*c*), which is a known spectral absorption recently investigated using CW photomixer techniques [21] (we find a similar line-width to the CW technique using this on-chip method technique – see [19] for a fuller comparison of the two techniques). We note that free-space THz-TDS spectra of a much larger ($\sim$0.1 cm^{-3}) sample (Fig. 1*c*) showed the same resonance, albeit with a poorer frequency resolution. Interestingly, it is not necessary for any part of the on-chip system to be in contact with the sample to obtain such absorption data. Fig. 1*d* shows the depth of the absorption feature as the separation between the microstrip and the lactose sample is adjusted, for a range of different bias voltages applied to the emitter (the emitter bias controls the strength and spatial extent of the evanescent electric field above the chip); we are able to resolve the absorption resonance for separations as large as 60 μm.

There are several conclusions we may draw from such on-chip spectroscopic data. First, the modal volume of the electric field above the microstrip interacting with the sample, which is of the order of 10^{-13} m^3, is approximately one thousandth of that used in a typical free-space spectroscopy experiment, yet the absorption feature is similarly pronounced in the data. This bodes well for the use of on-chip systems in applications where the available sample volume is very small (such as protein crystals, and other biological samples which are of similar size or smaller than the THz wavelengths involved). Secondly, since absorption resonances can be observed even when the waveguide is not in direct contact with the sample, this form of THz spectroscopy may be robust enough to be used in the development and spectroscopy of pharmaceutical drugs, for example, where its high spectral sensitivity and frequency resolution are also relevant. The range of potential applications could be greatly enhanced if its (currently somewhat limited) bandwidth of $\sim$1.5 THz can be extended to the several THz range, by further optimisation of the photoconductive materials, or by the use of lower-loss dielectric materials, for example. The use of other related waveguides, such as the Goubau-line [17], may also enhance bandwidth.

Imaging: The second experiment which we discuss involves the addition of passive bandstop filters to an on-chip microstrip system, otherwise similar to that discussed above; the filters act as sensitive probes of their dielectric environment, allowing a THz microscopy modality. In a 2002 paper [20], Nagel *et al.* demonstrated the use of bandpass filters embedded in a microstrip system to sense their local dielectric environment, showing that the frequency of the filter could be used to sense the difference in permittivity between single-stranded and hybridised DNA samples, for example. In later work, we showed that more compact bandstop THz filters could be formed in microstrip [11], and that their sensitivity to dielectric loading (in terms of frequency shift per unit active area of the passive filter) was rather better [16, 22]. The

experimental results on frequency shift of THz bandstop filters with overlaid dielectric showed excellent agreement with numerical simulations in which there are no free parameters [16] (we determined accurate values for the permittivity of the dielectric used in our simulation from independent THz-TDS experiments). Confirming from these simulations that, on-resonance, bandstop THz filters show a concentration of electric field at their tip (as expected from gigahertz bandstop filters, which have similar though larger geometries), we were encouraged to develop a sensitive terahertz microscope which uses these filters as the scanning tip.

In the following work, we used two bandstop stub filters, one designed to provide bandstop filtering centred at 600 GHz, and the second at 260 GHz, which were both attached to the same microstrip-line. The experimental arrangement, shown in Fig. 2*a* is similar, in terms of THz excitation and detection, to the spectroscopy experiment described above, but the addition of the two bandstop filters causes the frequency spectrum of the transmitted pulses to develop two sharp dips, each centred at the centre frequency of one filter (and, within our bandwidth, we also observe the third harmonic of the longer filter). The frequency of these absorptions depends on the dielectric environment of the filter, rather than the environment of the microstrip-line to which it is attached, with the largest shifts in frequency being produced by dielectric materials placed close to the end of a stub, where the electric field is concentrated. The independence of the frequency shift caused by loading each stub was demonstrated [16] by loading each filter in turn with a dielectric material (a photoresist); dielectrics surrounding one stub were found not to affect the frequency response of the other stub.

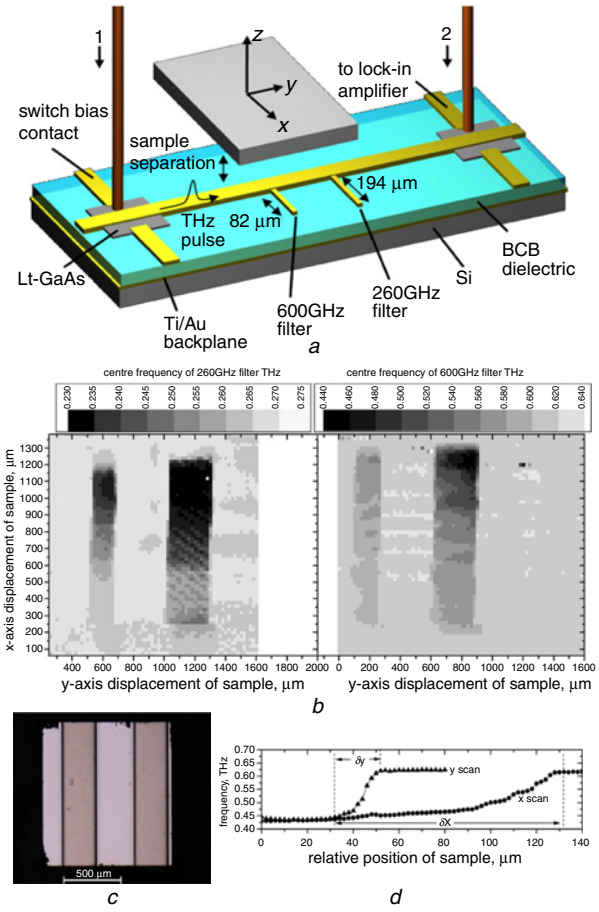

Fig. 2 *Schematic diagram of guided-wave THz microstrip circuit probing a GaAs dielectric sample; images obtained by raster scanning etched GaAs sample; optical micrograph of etched sample scanned in Fig. 2b, for comparison; line scan of edge of GaAs sample, demonstrating resolution of y- and x-direction*

a Schematic diagram of guided-wave THz microstrip circuit probing a GaAs dielectric sample (not to scale).
GaAs samples were mounted onto coupled stack of *x*,*y*,*z* piezoelectric translation stages, allowing accurate (submicron) positioning of samples with respect to THz circuit.
b Images obtained by raster scanning etched GaAs sample above circuit and extracting frequency shift of each filter for each spatial position of sample.
c Optical micrograph of etched sample scanned in Fig. 2*b*, for comparison.
d Line scan of edge of GaAs sample, demonstrating resolution of ~20 μm in *y*-direction, and ~100 μm in *x*-direction.

In order to achieve imaging, we bring objects into the evanescent field of the microstrip, and measure the time-domain response of the system, which we then Fourier transform, to extract the frequency response of both filters. By raster scanning an object parallel to the chip surface, and within the evanescent field extending above each filter, we can plot the centre frequency of each filter, and use it to reconstruct a THz image of the object. To demonstrate this imaging modality, we refer to Fig. 2*b*, which shows a greyscale image of a semiconductor etched into stripes and brought into the evanescent field above the filters, with image contrast being obtained from changes in the size of the frequency shift as the semiconductor is moved. When the raised regions of the semiconductor surface are close to a filter, a large shift in frequency response is found. To investigate the spatial resolution of the technique, we show in Fig. 2*c* line scans of the etched semiconductor surface profile, for movement of the sample along the *x*- and *y*-directions (see Fig. 2*a*). The spatial resolution is ~100 μm in *x* and 20 μm in *y*. The *y* resolution could be improved by using a filter with smaller width (our filter had a width of ~5 μm) and/or a thinner dielectric to restrict the extent of the evanescent field, but the *y* resolution is set by the length of the filter, which also determines its fundamental frequency, and is therefore difficult to reduce.

In principle, this imaging modality could provide quantitative information about local permittivity of materials over sub-wavelength length-scales, but this requires three-dimensional numerical modelling to form a link between the size of frequency shift recorded at each filter, and a (known) geometry being scanned. It would not be possible to determine the permittivity of an unknown arbitrary geometry, for example, since the effect of a reduction in permittivity (a reduction in filter centre frequency) is equivalent to the effect of increasing the separation between the sample and the filter, such as might be caused by a recess on the sample. Linking the technique to a surface profiling modality such as atomic force microscopy (AFM) could overcome this limitation.

The imaging modality appears to have two other limitations; only two frequencies are proved simultaneously, and objects must be planar so that in raster scanning them above the chip surface they cannot crash into the chip surface. Neither of these limitations is very fundamental. An array containing many (10 or more) filters is possible with the presented simple bandstop filter design, each sampling a different frequency within the ~1.5 THz bandwidth of the system. The total number of filters which could be usefully used is limited by the necessity to distinguish the individual response of each filter in the Fourier transform, and therefore by the bandwidth of each filter.

The second limitation, that of the overall planarity to the sample, could be removed by the use of other waveguides which would allow non-planar resonators to be attached to the signal conductor (such 'tips' being easier to scan around complex sample geometries than the planar geometry of our waveguide with its attached filters). The radial field mode which extends around Goubau-line on-chip waveguides [17] is particularly well suited to the integration of non-planar filters (such as could be formed from a cylinder or cone extending above the centre conductor), though simulations indicate that such filters should make only a small angle with the substrate to generate a large enough interaction with the propagating electric field. As mentioned above, integration of such waveguides with atomic force microscopy (AFM) can be envisaged, so that 2D topological mapping in the usual AFM modality could be combined with (perhaps fibre-coupled) on-chip measurements of THz dielectric permittivity. We note that a conceptually similar arrangement allowing microwave frequency range measurements of capacitance combined with simultaneous AFM measurements has recently been demonstrated by Agilent Technologies.

Conclusion and future directions: In this Letter, we have briefly reviewed the status of on-chip pulsed terahertz systems, and their application in spectroscopy and imaging experiments. We turn now to some potential future applications. The demonstrated ability to confine THz radiation to length-scales well below the diffraction limit may potentially provide a method to investigate the THz response of individual nanostructures (rather than ensembles of such systems, which are familiar from many THz/FIR experiments). An intriguing experiment in 2004 by Shaner and Lyon at Princeton University [23] showed that one could detect the transport of few-picosecond current pulses, generated in a coplanar waveguide, through a two-dimensional electron gas formed in a GaAs/AlGaAs heterostructure. Though the resulting current pulse showed dramatic dispersion, it was possible to distinguish

it above the background signal, demonstrating for the first time that on-chip pulsed THz systems could be used for the measurement of individual semiconductor nanostructures. It is interesting to note that the cutoff frequency both of one-dimensional semiconductor systems [24], and of graphene systems [25], is predicted to occur at or above THz frequencies, and that a similar coupling of few-picosecond duration pulses from on-chip waveguides could provide a realistic methodology for measuring their frequency response, and potentially their dynamic conductivity at THz frequencies. The recent demonstration of an optical quantum Hall effect at THz frequencies (using free-space THz-TDS) [26] underlines that there is interesting physics to be investigated by combining mesoscopic physics experiments with pulsed THz techniques. We have already shown that the responses of on-chip THz systems suffer no degradation at cryogenic (4K) temperatures [27], and given the laser power levels required for on-chip measurements are <1 mW, which is compatible with the cooling power available from dilution refrigeration, it seems likely that on-chip systems could become useful tools for the investigation of the THz response of individual nanostructures in the strong quantum regime of low temperatures and high magnetic fields.

Acknowledgments: The authors acknowledge the many discussions and ongoing collaboration with A. G. Davies and E. H. Linfield, and acknowledge S. Khanna and L. Li for the growth of LT-GaAs at the University of Leeds MBE facility. The authors gratefully acknowledge funding by the EPSRC, the Leverhulme Trust (grant ref. F/00 122/AM), and the Agilent Foundation.

5 October 2010
doi: 10.1049/el.2010.3317

J. Cunningham, M.B. Byrne, C.D. Wood and L. Dazhang (*School of Electronic and Electrical Engineering, University of Leeds, Woodhouse Lane, Leeds LS2 9JT, United Kingdom*)

E-mail: j.e.cunningham@leeds.ac.uk

References

1 Hu, B.B., and Nuss, M.C.: 'Imaging with terahertz waves', *Opt. Lett.*, 1996, **20**, p. 1716
2 Mittleman, D.M., Jacobsen, R.H., and Nuss, M.C.: 'T-ray imaging', *IEEE J. Sel. Top. Quantum Electron.*, 1996, **2**, p. 679
3 Wu, Q., and Zhang, X.-C.: 'Ultrafast electo-optic field sensors', *Appl. Phys. Lett.*, 1996, **68**, p. 1604
4 Fan, W.H., Burnett, A., Upadhya, P.C., Cunningham, J., Linfield, E.H., and Davies, A.G.: 'Far-infrared spectroscopic characterisation of explosives for security applications using broadband terahertz time-domain spectroscopy', *Appl. Spectrosc.*, 2007, **61**, p. 638
5 Wood, C.D., Hatem, O., Cunningham, J.E., Linfield, E.H., Davies, A.G., Cannard, P.J., Robertson, M.J., and Moodie, D.G.: 'Terahertz emission from metal-organic chemical vapor deposition grown Fe:InGaAs using 830 to 1.55 μm excitation', *Appl. Phys. Lett.*, 2010, **96**, p. 194104
6 Auston, D.H., Johnson, A.M., Smith, P.R., and Bean, J.C.: 'Picosecond optoelectronics detection, and correlation measurements in amorphous semiconductors', *Appl. Phys. Lett.*, 1980, **47**, p. 371
7 Mendis, R., and Grischkowsky, D.: 'Undistorted guided-wave propagation of subpicosecond pulses', *Opt. Lett.*, 2001, **26**, p. 846
8 Nagel, M., Dekorsky, T., Brucherseiferm, M., Haring Bolivar, P., and Kurz, H.: 'Characterisation of polypropylene thin-film microstrip at millimeter and sub-millimeter wavelengths', *Microw. Opt. Technol. Lett.*, 2001, **29**, p. 97
9 Yablonovitch, E., Hwang, D.M., Gmitter, T.J., Florez, L.T., and Harbinson, J.P.: 'Van der Waals bonding of GaAs epitaxial lift-off films onto arbitrary substrates', *Appl. Phys. Lett.*, 1990, **56**, p. 2419
10 Gregory, I.S., Baker, C., Tribe, W.R., Evans, M.J., Beere, H.E., Linfield, E.H., Davies, A.G., and Missous, M.: '100 fs annealed low-temperature-grown GaAs', *Appl. Phys. Lett.*, 2003, **83**, p. 4199
11 Cunningham, J., Wood, C.D., Davies, A.G., Hunter, I.C., Linfield, E.H., and Beere, H.E.: 'Terahertz frequency range band-stop filters', *Appl. Phys. Lett.*, 2005, **86**, p. 213503
12 Wang, K.L., and Mittleman, D.M.: 'Metal wires for terahertz wave guiding', *Nature*, 2004, **432**, pp. 376–379
13 Melinger, J.S., Laman, N., Harsha, S.S., and Grischkowsky, D.: 'Line-narrowing of terahertz vibrational modes for organic thing polycrystalline films within a parallel plate waveguide', *Appl. Phys. Lett.*, 2006, **89**, p. 251110
14 Yeh, C., Shimabukuro, F., and Seigel, P.H.: 'Low loss terahertz ribbon waveguides', *Appl. Opt.*, 2005, **44**, p. 5937
15 McGowan, R.W., Grischkowsky, D., and Misewich, J.A.: 'Demonstrated low radiative loss of a quadrupole ultrashort electrical pulse propagated on a three strip coplanar transmission line', *Appl. Phys. Lett.*, 1997, **71**, p. 2842
16 Cunningham, J., Wood, C., Davies, A.G., Tiang, C.K., Evans, D.A., Linfield, E.H., and Hunter, I.C.: 'Multiple frequency pulsed sensing of dielectric films', *Appl. Phys. Lett.*, 2006, **88**, p. 071112
17 Dazhang, L., Cunningham, J., Byrne, M.B., Khanna, S., Wood, C.D., Burnett, A.D., Ershad, S.M., Linfield, E.H., and Davies, A.G.: 'On-chip terahertz Goubau-line waveguides with integrated photoconductive emitters and mode-discriminating detectors', *Appl. Phys. Lett.*, 2009, **95**, p. 092903
18 Cunningham, J., Byrne, M., Upadhya, P., Lachab, M., Linfield, E.H., and Davies, A.G.: 'Terahertz evanescent field microscopy of dielectric materials using on-chip waveguides', *Appl. Phys. Lett.*, 2008, **92**, p. 032903
19 Bryne, M.B., Cunningham, J., Tych, K., Burnett, A.D., Stringer, M.R., Wood, W.D., Dazhang, L., Lachab, M., Linfield, E.H., and Davies, A.G.: 'Terahertz vibrational absorption spectroscopy using microstrip-line waveguides', *Appl. Phys. Lett.*, 2008, **93**, p. 182904
20 Nagel, M., Haring Bolivar, P., Brucherseifer, M., Kurz, H., Bosserhoff, A., and Buttner, R.: 'Integrated THz technology for label-free genetic diagnosis', *Appl. Phys. Lett.*, 2002, **80**, p. 154
21 Brown, E.R., Bjarnason, J.E., Fedor, A.M., and Korter, T.M.: 'On the strong and narrow absorption signature in lactose at 0.53 THz', *Appl. Phys. Lett.*, 2007, **90**, p. 061908
22 Tiang, C.K., Cunningham, J., Wood, C., Hunter, I.C., and Davies, A.G.: 'Electromagnetic simulation of terahertz frequency range filters for genetic sensing', *J. Appl. Phys.*, 2006, **100**, p. 066105
23 Shaner, E.A., and Lyon, S.A.: 'Picosecond time-resolved two-dimensional ballistic electron transport', *Phys. Rev. Lett.*, 2004, **93**, p. 037402
24 Kelly, M.J., Brown, R.J., Smith, C.G., Wharam, D.A., Pepper, M., Ahmed, H., Hasko, D.G., Peacock, D.C., Frost, J.E.F., Newbury, R., Ritchie, D.A., and Jones, G.A.C.: 'One-dimensional ballistic resistor in hot-electron regime: nonlinear and negative differential resistance to 10 THz', *Electron. Lett.*, 1989, **25**, pp. 992–993
25 Lin, Y.-M., Jenkins, K.A., Valdes-Garcia, A., Small, J.P., Farmer, D.B., and Avouris, P.: 'Operation of graphene transistors at gigahertz frequencies', *Nano Lett.*, 2009, **9**, pp. 422–426
26 Ikebe, Y., Moromoto, T., Masutomi, R., Okamoto, T., Aoki, H., and Shimano, R.: 'Optical Hall effect in the integer quantum Hall regime', *Phys. Rev. Lett.*, 2010, **104**, p. 256802
27 Wood, C., Cunningham, J., Upadhya, P.C., Linfield, E.H., Hunter, I.C., Davies, A.G., and Missous, M.: 'On-chip photoconductive excitation and detection of pulsed terahertz radiation at cryogenic temperatures', *Appl. Phys. Lett.*, 2006, **88**, p. 142103